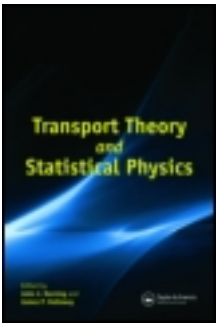

Transport Theory and Statistical Physics
Publication details, including instructions for authors and subscription information:
http://www.tandfonline.com/loi/ltty20

Kinetic and viscous boundary layers for broadwell equations

Jian-Guo Liu [a] & Zhouping Xin [b]
[a] Dept of Mathematics , Temple University , Philadelphia, PA, 19122
[b] Courant Institute , 251 Mercer Street, New York, NY, 10012
Published online: 20 Aug 2006.

To cite this article: Jian-Guo Liu & Zhouping Xin (1996) Kinetic and viscous boundary layers for broadwell equations, Transport Theory and Statistical Physics, 25:3-5, 447-461, DOI: 10.1080/00411459608220713

To link to this article: http://dx.doi.org/10.1080/00411459608220713

TRANSPORT THEORY AND STATISTICAL PHYSICS, 25(3-5), 447-461 (1996)

KINETIC AND VISCOUS BOUNDARY LAYERS FOR BROADWELL EQUATIONS

Jian-Guo Liu
Dept of Mathematics
Temple University
Philadelphia, PA 19122

Zhouping Xin
Courant Institute
251 Mercer Street
New York, NY 10012

Abstract

In this paper, we investigate the boundary layer behavior of solutions to the one dimensional Broadwell model of the nonlinear Boltzmann equation for small mean free path. We consider the analogue of Maxwell's diffusive and the reflexive boundary conditions. It is found that even for such a simple model, there are boundary layers due to purely kinetic effects which cannot be detected by the corresponding Navier-Stokes system. It is also found numerically that a compressive boundary layer is not always stable in the sense that it may detach from the boundary and move into the interior of the gas as a shock layer.

1. INTRODUCTION

We investigate the boundary layer behavior of the solutions to the one dimensional Broadwell model [1] of the nonlinear Boltzmann equation with analogue of Maxwell's diffusive and diffusive-reflexive boundary conditions at small mean free path. The general Boltzmann equation of kinetic theory gives a statistical description of a gas of interacting particles. An important property of this equation is its asymptotic equivalence to the Euler or Navier-Stokes equations of the compressible fluid dynamics, in the limit of small mean free path. One expects that away from initial, boundary, and shock layers, the Boltzmann solution should relax to its equilibrium state (local Maxwellian state) in the limit of small mean free path, and the gas should be governed by the macroscopic fluid equations as suggested by Hilbert and the Chapman-Enskog expansions [2]. Both the formal and rigorous mathematical justification of the fluid-dynamic approximations of Boltzmann solutions pose challenging open problems in most physically interesting cases. Most of the work in the literature concentrate on the initial layer problems for some models and general Boltzmann equation [3,4,5,6] with notable exceptions [7,8,9]. The asymptotic behavior at small mean free path of solutions to the Boltzmann equation in the presence of shocks or boundaries remains far from being well-understood (not even formally), but see ([10,11]). In particular, for the boundary layer problem, a qualitative theory

exists for some models of steady Boltzmann equations [2], but very little is known for the unsteady problems. Since boundary layers are important due to the fact that they describe the interactions of the gas molecules with the molecules of the solid body, to which one can trace the origin of the drag exerted by the gas on the body and the heat transfer between the gas and the solid boundaries, it is very important to understand the asymptotic behavior of the microscopic quantities when there are interactions of the gas with solid boundaries. It is expected that the fluid approximation is still valid away from the boundary. One of the difficulties in analyzing this problem is due to the complexity of the nonlocal collision operator in the Boltzmann equation which makes it difficult to study the structures of the layer problems associated with the formal matched asymptotic analysis. Furthermore, even in the case that the structures of these layers are relatively easy to study as for the Broadwell model, the fluid dynamic approximation cannot be obtained easily due to the stiffness of the limit and weaker dissipation mechanism.

In this paper, we address the boundary layer problem for the much simpler one dimensional Broadwell model of the nonlinear Boltzmann equation. We will consider the analogue of the Maxwell's diffusive and diffusive-reflexive boundary conditions. As a continuation of [12] in which we have classified the boundary layers as either expansive or compressive (see also §2.3), and shown that the boundary layers are nonlinearly stable and the layer effects are localized so that the fluid-dynamics approximation is valid away from the boundary provided that the boundary layer exists, here first we report some numerical experiments which show surprisingly that for both diffusive and diffusive-reflexive boundary conditions, a compressible boundary layer is not always stable in the sense that it may detach from the boundary and move into the interior of the gas as a shock layer, which we call boundary induced shocks (see §3). We will also show rigorously that even for such a simple model, there exist boundary layers due to purely kinetic effects which can not be detected by the Chapman-Enskog expansion on the viscous level. This phenomena was observed previously in the steady problems for the GBK model [2]. We should remark that the phenomena of detachment of a compressive boundary layer and the resulting induced shock layer is very surprising to us. It will be interesting to find out whether this happens for other more practical models of the Boltzmann equation [6].

The rest of the paper runs as follows. In §2, the initial boundary valued problems for the Broadwell model and the corresponding model Euler equations are formulated. We then solve the boundary layer equations and classify the boundary layer in terms of the rate of change of the associated characteristic speeds. The numerical experiments which show the detachment of a compressive boundary layer is described in detail in §3. Finally, we show that there are Broadwell boundary layers which cannot be detected by the model Navier-Stokes equations derived by the Chapman-Enskog expansion. This is given in §4.

2. BOUNDARY LAYERS FOR THE BROADWELL MODEL

2.1. Initial-Boundary Value Problems for the Broadwell Model and the Corresponding Fluid Equations

The Broadwell model describes a gas as composed of particles of only six speeds

with a binary collision law and spatial variation in only one direction. In one space dimension, the model takes the following form [1]

$$\begin{cases} \partial_t f^+ + \partial_x f^+ = \frac{1}{\varepsilon}(f^0 f^0 - f^+ f^-)\,, \\ \partial_t f^0 \qquad\quad = \frac{1}{2\varepsilon}(f^+ f^- - f^0 f^0)\,, \\ \partial_t f^- - \partial_x f^- = \frac{1}{\varepsilon}(f^0 f^0 - f^+ f^-)\,, \end{cases} \tag{2.1}$$

where ε is the mean free path, f^+, f^0, and f^- denote the mass densities of gas particle with speed 1, 0 and -1, respectively. In what follows, we will use the vector notation $\mathbf{f} = (f^+, f^0, f^-)$. The fluid moments are defined as:

$$\rho = f^+ + 4f^0 + f^-\,, \quad m = f^+ - f^-\,, \quad u = \frac{m}{\rho} \tag{2.2}$$

which are hydrodynamical quantities; the mass density, momentum, and fluid velocity respectively. The state $\mathbf{f}$ is said to be a local Maxwellian [13] if

$$\rho > 0\,, \qquad |u| < c\,, \quad \text{and} \quad f^+ + f^- = \rho\sigma(u)\,, \tag{2.3}$$

where

$$\sigma(u) = \frac{2}{3}\sqrt{1 + 3u^2} - \frac{1}{3}\,. \tag{2.4}$$

By assuming the state is in equilibrium, one has

$$\begin{cases} \partial_t \rho + \partial_x(\rho u) = 0\,, \\ \partial_t(\rho u) + \partial_x(\rho\sigma(u)) = 0\,, \end{cases} \tag{2.5}$$

which is called the model Euler equation that shares many properties of the isentropic gas dynamics when the macroscopic speed of the gas is relatively small compared with the microscopic speed of the gas particles [13]. The system (2.5) is strictly hyperbolic and genuinely nonlinear with characteristic speeds,

$$\lambda_1 = 2\frac{u - \sqrt{\sigma(u)}}{3\sigma(u) + 1} \quad \text{and} \quad \lambda_2 = 2\frac{u + \sqrt{\sigma(u)}}{3\sigma(u) + 1}\,, \tag{2.6}$$

satisfying

$$-1 < \lambda_1(u) < 0 < \lambda_2(u) < 1\,, \quad \text{if } |u| < 1\,, \tag{2.7}$$

and

$$\frac{d\lambda_i(u)}{du} > 0\,, \quad i = 1, 2\,. \tag{2.8}$$

Using the Chapman-Enskog expansion [13], one can derive that the first order approximation of the Broadwell equations is the following model Navier-Stokes equations

$$\begin{cases} \partial_t \rho + \partial_x(\rho u) = 0\,, \\ \partial_t(\rho u) + \partial_x(\rho\sigma(u)) = \varepsilon\partial_x(\mu(u)\partial_x u)\,, \end{cases} \tag{2.9}$$

here

$$\mu(u) = \frac{2\big(1-\sigma(u)\big)}{(1+3u^2)^{3/2}}\,. \tag{2.10}$$

We will consider the Broadwell equations on the region

$$\Omega_T = \big\{(x,t)\,,\quad s(t) \le x < +\infty,\quad 0 \le t \le T\big\}\,, \tag{2.11}$$

with the moving boundary given by

$$x = -\alpha t = s(t)\,. \tag{2.12}$$

To simplify the presentation, we assume $0 < \alpha < 1$. We remark here that the cases $\alpha = 0$ and $\alpha = 1$ correspond to the uniform characteristic boundary conditions for the Broadwell equations, in which there are no strong boundary layers so that the fluid dynamic approximation can be easily justified.

The initial data for (2.1) is

$$(f^+, f^0, f^-)(x, t=0) = (f^+_{\rm in}, f^0_{\rm in}, f^-_{\rm in})(x) \tag{2.13}$$

Two types of boundary conditions will be considered. One is a purely diffusive boundary condition

$$f^+\big(s(t),t\big) = f^+_{\rm b}(t)\,, \qquad f^0\big(s(t),t\big) = f^0_{\rm b}(t)\,. \tag{2.14}$$

The other type is a diffusive-reflexive boundary condition

$$f^+\big(s(t),t\big) = a(t) f^-\big(s(t),t\big)\,, \qquad 4f^0\big(s(t),t\big) = b(t) f^-\big(s(t),t\big) \tag{2.15}$$

where a and b are positive functions. In particular, the purely reflexive boundary condition corresponds to taking a and b in (2.15) such that

$$a + \alpha(1 + a + b) = 1\,.$$

In this case, the mass flux is conserved on the boundary.

The gas near the boundary in general is not in equilibrium state. In order to understand the leading order behavior of the kinetic boundary layer, one can use the stretched variable $\xi = \frac{x+\alpha t}{\epsilon}$ and look for the solution to (2.1) of the form $\mathbf{f}(\xi,t) = \mathbf{f}(\frac{x+\alpha t}{\epsilon}, t)$. Simple calculations show that up to the leading order, the solution is governed by the following system of ordinary differential equations regarding t as parameter,

$$\mathrm{Diag}\,\big(\alpha+1\,,\,-2\alpha\,,\,\alpha-1\big)\frac{d\mathbf{f}}{d\xi} = (f^0 f^0 - f^+ f^-)(1,1,1)\,. \tag{2.16}$$

Corresponding to (2.14), the boundary data for (2.16) at $\xi = 0$ is given by

$$f^+(0) = f^+_{\rm b}\,,\ f^0(0) = f^0_{\rm b}\,, \tag{2.17}$$

while for (2.15), the boundary condition for (2.16) takes the form

$$f^+(0) - a f^-(0) = 0\,,\ 4f^0(0) - b f^-(0) = 0\,. \tag{2.18}$$

The state at $\xi = +\infty$ is in the fluid region hence taken to be a local Maxwellian in both cases,

$$\mathbf{f}_\infty = (f_\infty^+, f_\infty^0, f_\infty^-), \qquad f_\infty^+ f_\infty^- = (f_\infty^0)^2. \tag{2.19}$$

(2.16) is an integrable system, and the solutions can be found explicitly. As a consequence, one can obtain the appropriate boundary condition for the model Euler equation (2.5) as follows.

We start with the case associated with the diffusive boundary condition (2.14). It follows from (2.16) that there exist two functions $c_1(t)$ and $c_2(t)$ independent of ξ such that

$$(\alpha+1)f^+ + 2\alpha f^0 = c_1(t), \quad (\alpha-1)f^- + 2\alpha f^0 = c_2(t). \tag{2.20}$$

Using the boundary condition (2.17) leads to

$$c_1(t) = (\alpha+1)f_{\mathrm{b}}^+ + 2\alpha f_{\mathrm{b}}^0. \tag{2.21}$$

On the other hand, the boundary condition (2.19) yields

$$c_1(t) = \frac{\rho_{\mathrm{b}}}{2}\big((\alpha+1)\big(u_{\mathrm{b}} + \sigma(u_{\mathrm{b}})\big) + \alpha(1-\sigma(u_{\mathrm{b}}))\big), \tag{2.22}$$

where we have rewritten (2.19) in terms of the fluid moments. Setting

$$\mathcal{B}(\rho,u)(t) \equiv \tfrac{1}{2}\rho\big(\sigma(u) + (\alpha+1)u + \alpha\big)\,\big|_{(s(t),t)}, \tag{2.23}$$

we arrive at the desirable boundary condition for the Euler equations (2.5) as

$$\mathcal{B}(\rho,u)(t) = (\alpha+1)f_{\mathrm{b}}^+(t) + 2\alpha f_{\mathrm{b}}^0(t). \tag{2.24}$$

Similarly, in the case with diffusive-reflexive boundary condition (2.15), one can obtains the boundary condition for (2.5) as

$$u\big(s(t),t\big) = u_{\mathrm{b}}(t). \tag{2.25}$$

where u_{b} solves

$$(\alpha+u_{\mathrm{b}})\big(1+a-\alpha(1-a)\big) = \big(\sigma(u_{\mathrm{b}}) + \alpha u_{\mathrm{b}}\big)\big(1-a-\alpha(1+a+b)\big). \tag{2.26}$$

In particular, for the purely reflexive boundary condition, one has that

$$u\big(s(t),t\big) = u_{\mathrm{b}}(t) = -\alpha.$$

The initial data for the Euler equations (2.5) is given by

$$(\rho,m)(x,0) = \big(f_{\mathrm{in}}^+ + 4f_{\mathrm{in}}^0 + f_{\mathrm{in}}^-, f_{\mathrm{in}}^+ - f_{\mathrm{in}}^-\big)(x) \tag{2.27}$$

It can be shown easily that the initial-boundary value problems (2.5), (2.27) and (2.24) or (2.25) are well posed at least locally in time. To see this, we first rewrite the fluid equations (2.5) in the characteristic form:

$$\begin{cases} \partial_t \phi_+ + \lambda_+ \partial_x \phi_+ = 0, \\ \partial_t \phi_- + \lambda_- \partial_x \phi_- = 0, \end{cases}$$

in which the functions $\phi_\pm$ are the Riemann invariants of the form

$$\phi_\pm(\rho, u) = \rho^2(\sigma(u) - u^2) \exp\left\{ \pm 2 \int_0^u \left(\frac{\sigma(w)}{1+3w^2} \right)^{1/2} \frac{dw}{\sigma(w) - w^2} \right\}.$$

Setting $\phi_\pm(x,t) = \phi_\pm(\rho(x,t), u(x,t))$, one obtains from direct computation that

$$\frac{\partial \mathcal{B}}{\partial \phi_+} > 0. \tag{2.28}$$

Thus the implicit function theorem implies that the inflow ϕ_+ can be represented in terms of a smooth function of the outflow ϕ_- and the given boundary values. Consequently, the initial value problems (2.5), (2.27) and (2.24) or (2.25) are well-posed. Furthermore, the unique solution is physical in the sense that the macroscopic density, $\rho(x,t)$, is positive at least locally in time. This follows from the positivity of $\rho(x,0)$ and the contraction argument.

2.2. Classifications of the Boundary Layers

To determine the structure of the boundary layer, we now solve explicitly the system of first order ordinary differential equations (2.16) with boundary condition (2.17) and (2.19) or (2.18) and (2.19). Substitute (2.20) into the second equation in (2.16) to get

$$\frac{df^0}{d\xi} = \frac{-(3\alpha^2+1)}{2\alpha(1-\alpha^2} \left((f^0)^2 - \frac{2\alpha(c_1+c_2)}{3\alpha^2+1} f^0 + \frac{c_1 c_2}{3\alpha^2+1} \right). \tag{2.29}$$

Define

$$f^0_{-\infty} = -f^0_\infty + \frac{2\alpha}{3\alpha^2+1}(u_b + \alpha)\rho_b, \tag{2.30}$$

where $(\rho_b, u_b) = (\rho, u)(s(t), t)$. Direct calculation shows that

$$f^0_\infty + f^0_{-\infty} = \frac{2\alpha(c_1+c_2)}{3\alpha^2+1}, \qquad f^0_\infty f^0_{-\infty} = \frac{c_1 c_2}{3\alpha^2+1}, \tag{2.31}$$

and so, (2.29) becomes

$$\frac{df^0}{d\xi} = -c_\alpha (f^0 - f^0_\infty)(f^0 - f^0_{-\infty}) \tag{2.32}$$

where $c_\alpha = \frac{3\alpha^2+1}{2\alpha(1-\alpha^2)}$. Solving above equation, we obtain that

$$f^0(\xi) - f^0_\infty = \frac{(f^0_b - f^0_\infty)(f^0_\infty - f^0_{-\infty}) e^{-c_\alpha (f^0_\infty - f^0_{-\infty})\xi}}{f^0_b - f^0_{-\infty} - (f^0_b - f^0_\infty) e^{-c_\alpha (f^0_\infty - f^0_{-\infty})\xi}}. \tag{2.33}$$

(2.33) and (2.20) give the corresponding formulas for f^+ and f^-. Our next lemma shows that the boundary layers approach the Maxwellian states exponentially fast as the fast variable goes to infinity.

Lemma. *If* $\lambda_1(u_b) < -\alpha$, *then* $f^0_{-\infty} < f^0_\infty$. *Furthermore, if* $f^0_b > f^0_{-\infty}$, *then we have*

$$|\mathbf{f}(\xi) - \mathbf{f}_\infty| \le C|f^0_b - f^0_\infty| e^{-C(f^0_\infty - f^0_{-\infty})\xi}. \tag{2.34}$$

The proof follows direct computation.

We remark here that for a given boundary data, the condition that $f^0_b > f^0_{-\infty}$ is automatically satisfied if α is suitably small.

We now turn to the classification of boundary layers. Even though the gas near boundary is not in equilibrium in general, it is appropriate to use the monotonicity of $\lambda_1(u)$ to describe the kinetic boundary layers. We will say that a boundary layers is *compressive* if $\frac{d\lambda_1}{d\xi} < 0$; and it is *expansive* if $\frac{d\lambda_1}{d\xi} \ge 0$.

Since the characteristic speeds are monotone functions of the macroscopic velocity u (c.f. (2.8)), it is clear that the classification of the boundary layer depends on the monotonicity of u along the boundary layer profile. Direct calculation using (2.16) shows that

$$\frac{du}{d\xi} = -\frac{4\rho_b(\alpha + u_b)}{(1-\alpha^2)\rho^2}\frac{df^0}{d\xi}. \tag{2.35}$$

It follows from this that there are four different cases depending on the speeds of the wall and the fluid:

	$\frac{df^0}{d\xi} < 0$	$\frac{df^0}{d\xi} > 0$
compressive layer ($\frac{d\lambda_1(u)}{d\xi} < 0$)	$u_b < -\alpha$	$u_b > -\alpha$
expansive layer ($\frac{d\lambda_1(u)}{d\xi} \ge 0$)	$u_b \ge -\alpha$	$u_b \le -\alpha$

Similarly one can study the boundary layers for the Navier-Stokes equations (2.9). Viscous boundary layers can also be classified as either compressive or expansive. However, one can prove that viscous boundary layers exist only when $u_b > -\alpha$, see §4. It is very interesting to note that boundary layers, corresponding to $u_b \le -\alpha$, are purely due to the kinetic effects, which cannot be detected by the Chapman-Enskog expansions. This phenomena was observed previously in the steady problems for the GBK model (cf. [2]).

3. BOUNDARY INDUCED SHOCKS

Now we describe an interesting observation on the bifurcation of boundary layers for the Broadwell model. By numerical experiments, we show that the compressive

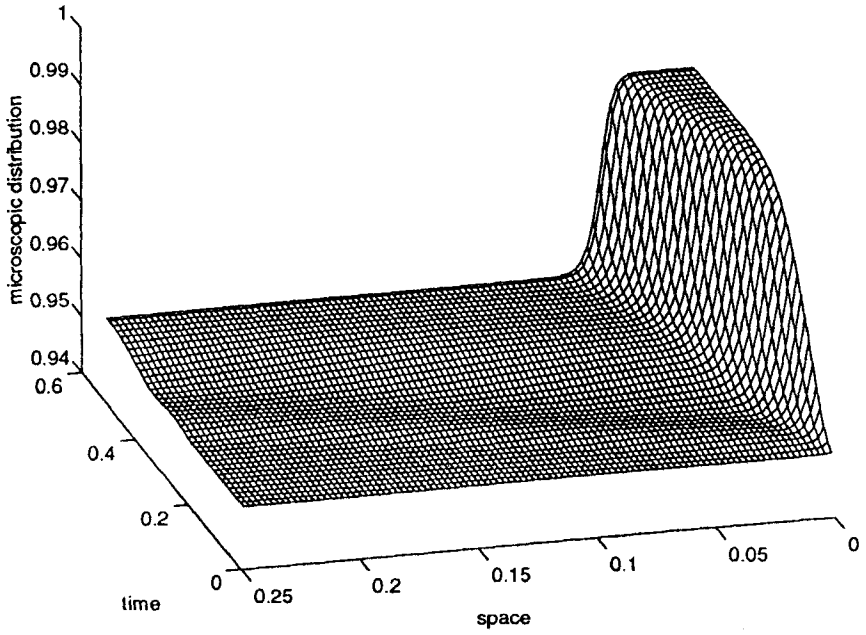

Figure 1. Compressive Boundary Layer. The evolution of the microscopic distribution of f^0 from time $t = 0$ to $t = 0.6$. The mean-free-path and the wall speed are taken to be .002 and -0.2, respectively. The boundary data is given by (3.1).

boundary layers may detach from the boundary wall at some time and move into the gas as fluid shocks, which we will call *boundary induced shocks*. This demonstrates that the compressive boundary layers may not be stable and furthermore they may affect the gas flow through compressive shocks. On the formal level, the bifurcation time is when the boundary data f_b^0 approaches $f_{-\infty}^0$ defined in (2.30).

In the following we explain the set up for the numerical experiments to demonstrate the formation of the compressive boundary layers and their bifurcation into shocks moving into the fluid region. The program can be easily reproduced on a small PC.

Our first numerical experiment is the detachment of the compressible boundary layer with the purely diffusive boundary conditions. To avoid the complications due to interactions among initial, boundary, and shock layers, and concentrate on the effects of boundary layers, we will use the Maxwellian state $f^+(x,0) = 0.95$, $f^0(x,0) = 0.2$, $f^-(x,0) = f^0(x,0)^2/f^+(x,0)$, for $0 < x < 1$ as initial microscopic distributions. The mean-free-path is taken to be 0.002 and the wall speed is taken to be $\alpha = 0.2$. The boundary data f_b^+ and f_b^0 are taken to be

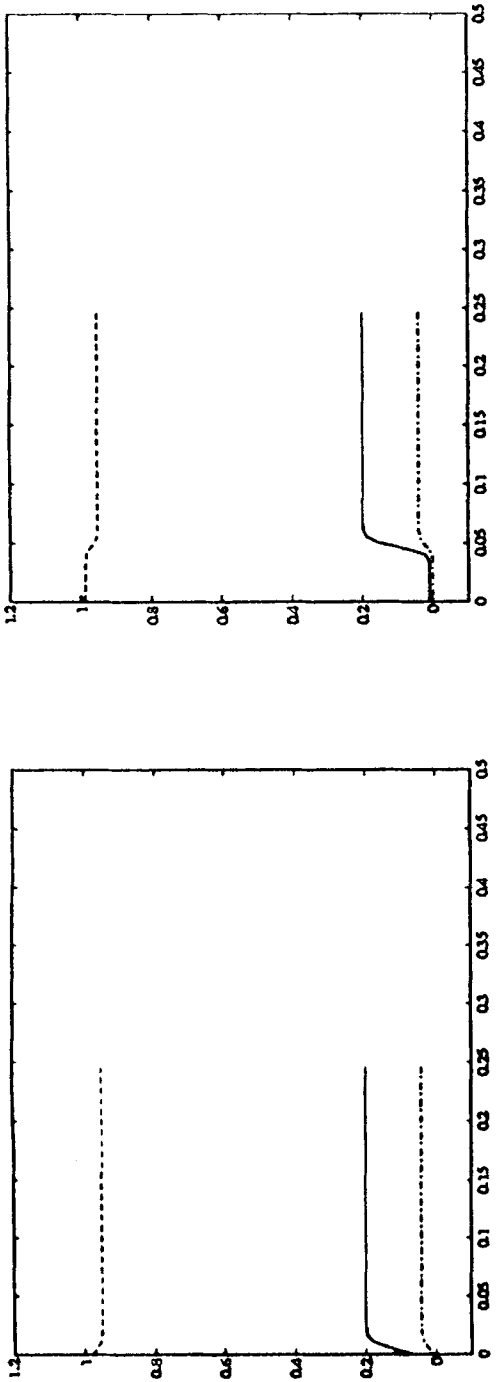

Figure 2. The horizontal axis represents the spatial scale. The solid, dashed, and dashdot lines denote the microscopic distribution of f^0, f^+, and f^-, respectively. (a) the boundary layer is formed at time = 0.16; (d) the boundary layer moved in the the interior of the gas at time = 0.6.

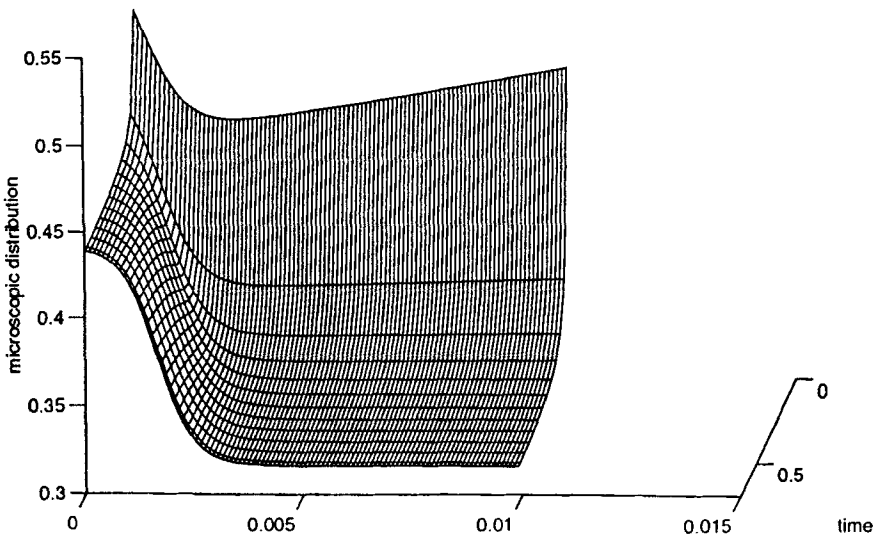

Figure 3. Compressive Boundary Layer with diffusive-reflexive boundary condition. The evolution of the microscopic distribution of f^0 from time $t = 0.3$ to $t = 0.4$. The mean-free-path and the wall speed are taken to be .001 and -0.3, respectively. The boundary data is given by (3.2).

$$f_b^+(t) = 0.988 - 0.038e^{-50t^2}, \qquad f_b^0(t) = 0.01 + 0.19e^{-50t^2}, \tag{3.1}$$

for the diffusive boundary condition. We note that the boundary data in (3.1) is chosen to be compatible with the initial data up to first order derivatives, so that there is no singularity formation at the corner.

The evolution from time $t = 0$ to $t = 0.6$ of the microscopic distribulation of f^+ is displayed in Figure 1. The formulation of the boundary layer and the detachment of the boundary layer can be seen clearly. The approximate solution to the Broadwell model is computed by a upwind scheme with space grid-size = 0.0005 and CFL number 0.7. The numerical boundary conditions at the right end are implemented by depleting the end values at every time step. The plots is in the moving coordinate.

To see this more clearly, we take two snapshots at time $t = 0.16$ and $t = 0.6$ and plot the distributions f^0, f^+, and f^- in Figure 2(a-b), respectively. These figures show that the compressible boundary layer has formed at time 0.16 (see Figure 2(b)) It is seen from Figure 2(d) that at the time = 0.6 the boundary layer has become a well resolved entropy shock and propagated into the fluids.

These phenomena also occur in the diffusive-reflexive boundary condition. Figure 3 displays the evolution the distribution f^+ from time $t = 0$ to $t = 0.7$ with the $a(t)$ and $b(t)$ in (2.15) taken as

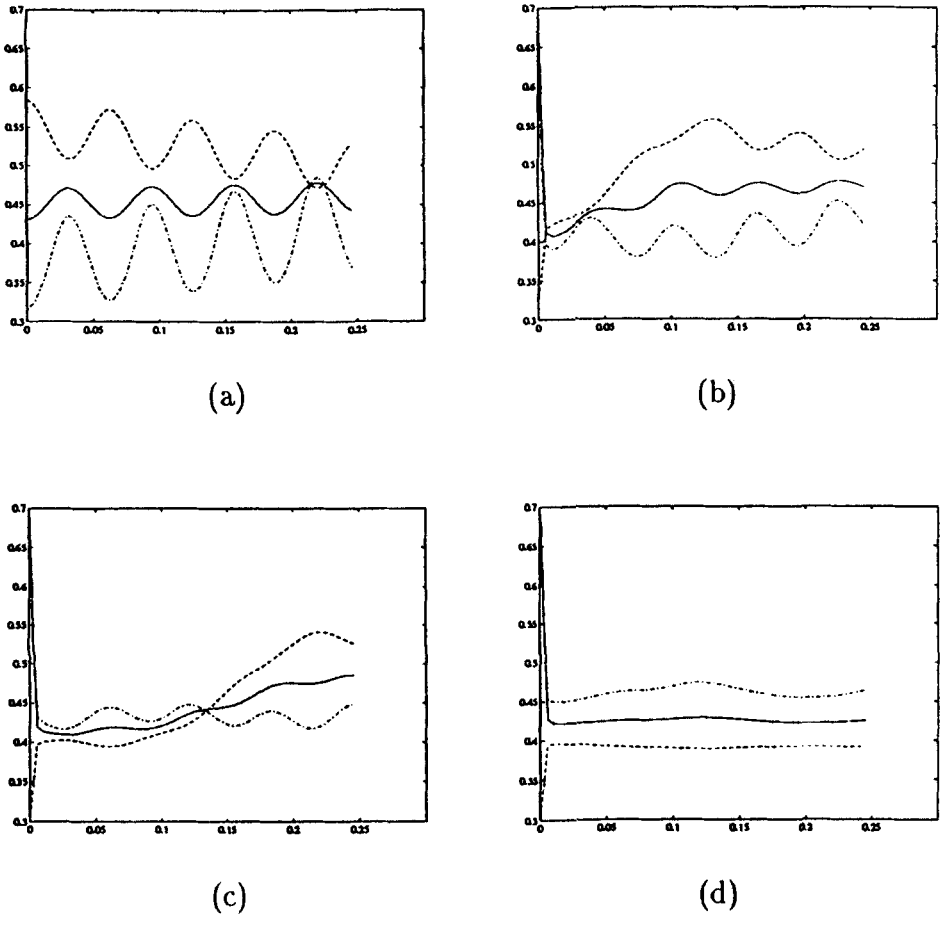

Figure 4. Expansive Boundary Layer. The solid, dashed, and dashdot lines represent the microscopic distributions, f^0, f^+, and f^-, respectively. Figure 4(a)-4(d) correspond to time $t = 0$, 0.16, 0.28, 0.6, respectively.

$$a(t) = a = 4.5918 + 200(1 - e^{-5t^2}), \qquad b(t) = 0.4357 + 0.1e^{-5t^2}. \tag{3.2}$$

The initial data is taken to a Maxwellian state $\mathbf{f}(x,0) = (0.75, 0.35, 0.1633)$, for $0 < x < 1$, the mean-free-path is taken to be 0.0001, and $\alpha = 0.3$, the space grid-size = 0.0001, and CFL number 0.7.

In Figure 4, we demonstrate the formation and stability of the expansive boundary layer through an example. In the numerical calculation, the mean-free path and the wall speed are taken to be 0.002 and -0.2, respectively, the initial data are

$$f^+(x,0) = 0.55 + 0.035\cos(100x) - 0.2x\,,$$
$$f^0(x,0) = 0.45 - 0.02\cos(100x) + 0.04x\,,$$
$$f^-(x,0) = f^0(x,0)^2/f^+(x,0)\,,$$

and the boundary data are given by

$$f_b^+(t) = 0.25 + 0.33e^{-100t^2}\,, \quad f_b^0(t) = 0.86 - 0.43e^{-100t^2}$$

Then Figure 4(a)-4(d) show the development of the boundary layer at the time sequence: $t = 0, 0.16, 0.28$ and 0.6, respectively. It should be clear that the boundary layer is attached to the boundary at all the time.

4. THE NAVIER-STOKES BOUNDARY LAYERS

In this section we will show that the boundary layers of Broadwell equations with property $u_b \le -\alpha$ are due to the kinetic effects only, which can not be detected by the first order viscous systems (2.9). Consider the Cauchy problem for (2.9) with initial data

$$\rho_\epsilon(x,0) = \rho^{in}(x)\,, \qquad m_\epsilon(x,0) = m^{in}(x)\,, \tag{4.1}$$

and boundary conditions

$$\rho_\epsilon(-\alpha t,t) = \rho^{bd}(t)\,, \qquad m_\epsilon(-\alpha t,t) = m^{bd}(t)\,. \tag{4.2}$$

Here the boundary data can be given explicitly in terms of those of the Broadwell equations and the solution to the initial-boundary value problem for the model Euler equations (2.5), (2.24). However, the specific form of the boundary data is irrelevant to our following analysis.

To study the boundary layer behavior of the solutions to the above viscous problem, we use the same stretched variable as before, i.e., $\xi = \frac{x+\alpha t}{\epsilon}$, and look for the solutions to (4.1) of the form $(\rho,u)(x,t) = (\rho,u)(\xi,t)$. Then up to the leading order, the boundary layer solutions should satisfy the following system of ordinary differential equations:

$$\begin{cases} \partial_\xi(\alpha\rho + m) = 0\,, \\ \partial_\xi(\alpha m + \rho\sigma(u)) = \partial_\xi(\mu(u)\partial_\xi u)\,. \end{cases} \tag{4.3}$$

The initial value of the boundary layer solution at $\xi = 0$ is given in (4.2), and its value at $\xi = \infty$ is

$$(\rho,u)(\infty,t) = (\rho_b,u_b)(t)\,, \tag{4.4}$$

where (ρ_b,u_b) is the boundary value of the solution to the model Euler equations (2.5).

Theorem. *There is no solution to the above problem* (4.2), (4.3) *and* (4.4), *if* $u_b \le -\alpha$.

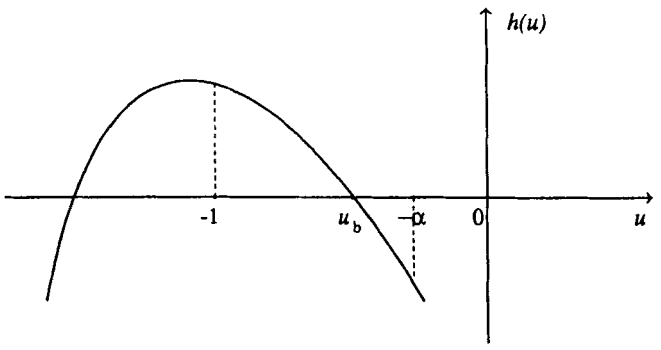

Figure 5.

Proof. Otherwise, one can integrate (4.3) to get that for some functions $c_3(t)$ and $c_4(t)$ independent of ξ such that

$$\begin{cases} \rho(u+\alpha) = c_3\,, \\ \rho\big(\alpha u + \sigma(u)\big) = \mu(u)\partial_\xi u - c_4\,. \end{cases} \tag{4.5}$$

or,

$$\frac{c_3}{u+\alpha}\big(\alpha u + \sigma(u)\big) + c_4 = \mu(u)\partial_\xi u\,. \tag{4.6}$$

Set

$$h(u) = c_3\big(\alpha u + \sigma(u)\big) + c_4(u+\alpha)\,. \tag{4.7}$$

One then integrates (4.5) to obtain that

$$\int_{u^{\rm bd}}^{u} \frac{\mu(u)(u+\alpha)}{h(u)}\,du = \xi > 0\,. \tag{4.8}$$

It thus suffices to show that in the case $u_b + \alpha < 0$, there exists no solution to the integral equation (4.8) such that

$$u \to u_b, \quad \text{as} \quad \xi \to \infty\,. \tag{4.9}$$

To this end, one notes that

$$h''(u) = c_3\sigma''(u) < 0\,,$$

and

$$h(-\alpha) = c_3\big(\sigma(\alpha) - \alpha^2\big) < 0\,,$$

since c_3 is negative. It is then clear that $h(u)$ has at most two roots. Now if we assume that there exist solutions to (4.8) with property (4.9), then both of the roots of $h(u)$ must lie on the left of $-\alpha$. Now we claim that

$$h(-1) = (1-\alpha)(c_3 - c_4) > 0 \tag{4.10}$$

so that there exists only one simple root in $(-1, -\alpha)$. In fact, if (4.10) fails, then $h(-1) \le 0$. This implies that $c_3 \le c_4$, i.e.,

$$c_4 = \frac{c_3(\alpha u_b + \sigma(u_b))}{-(\alpha + u_b)} \ge c_3$$

where one has used (4.6). Due to $c_3 < 0$, the above inequality is equivalent to

$$\alpha u_b + \sigma(u_b) + \alpha + u_b \le 0\,. \tag{4.11}$$

Set

$$f(u) = \alpha u + \sigma(u) + \alpha + u\,.$$

Easy computation shows that

$$f(-1) = 0\,, \qquad f'(-1) = \alpha > 0\,, \qquad f''(u) = \sigma''(u) > 0\,.$$

It follows that

$$f(u) > 0\,, \qquad \text{for } -1 < u < -\alpha\,,$$

which contradicts to (4.11). Finally, we show that the fact that there is one simple root in $(-1, -\alpha)$ gives the desired contradiction. Note that in our case that the simple root must be u_b. Then if $u^{bd} < u_b$, the integral on the left hand side of (4.8) is negative due to the fact that $h(u)$ must be positive in $(-1, u_b)$ which contradicts (4.8). Similarly one treats the case that $u^{bd} > u_b$. This completes the argument. We remark here that it is easy to check that our analysis also works for the case $u_b + \alpha = 0$. The proof of the Theorem is complete.

Acknowledgments: The research of J.-G.L. was supported in part by a NSF Grant DMS-9505275 and a summer research fellowship from Temple University, and the research of Z.X. was supported in part by a Sloan Foundation Fellowship, NSF Grant DMS-93-03887, and DOE Grant DE-FG02-88ER-25053.

REFERENCES

1. J.E. Broadwell, *Phys. Fluids* **7**, 1243–1247 (1964).
2. C, Cercignani, *The Boltzmann Equation and Its Applications*, Springer-Verlag, New York (1988).
3. R.E. Caflisch, *Comm. Pure Appl. Math.* **33**, 651–666 (1980).
4. H. Grad, "Singular and nonuniform limits of solutions of the Boltzmann equations" *SIAM-AMS Proceedings I, Transport Theory*, 296–308 (1969).

5. R.E. Caflisch and G.C. Papanicolaou, *Comm. Pure Appl. Math.* **32**, 589–616 (1979).
6. T. Platkowski and R. Illner, "Discrete velocity models of the Boltzmann equation: a survey on the mathematical aspects of the theory", *SIAM Rev.* **30**, 213–255 (1988).
7. C. Bardos, F. Golse and C.D. Levermore, *Comm. Pure Appl. Math.* **46**, 667–753 (1993).
8. M. Slemrod and A.E. Tzavaras, *Arch. Rational Mech. Anal.* **122**, 353-392 (1993).
9. C. Bardos, R. Caflisch and B. Nicolaenko, *Comm. Pure Appl. Math.* **39** (1986).
10. R.E. Caflisch and B. Nicolaenko, *Commun. Math. Phys.* **86**, 161–194 (1982).
11. Zhouping Xin, *Comm. Pure Appl. Math.* **44**, 679–713 (1991).
12. Jian-Guo Liu and Zhouping Xin, "Boundary Layer Behavior in the Fluid-Dynamic Limit for a Nonlinear Model Boltzmann Equation" *to appear in Arch. Rational Mech. Anal.* (1995)
13. R.E. Caflisch, *Comm. Pure Appl. Math.* **32**, 521–554 (1979).

Received: November 10, 1994
Revised: July 20, 1995
Accepted: November 17, 1995